*Egypt. J. Chem.* **Vol. 67**, No. 12 pp. 217 - 230 (2024)

**Egyptian Journal of Chemistry**

**http://ejchem.journals.ekb.eg/**

# Improving the Functional Properties of Egyptian Cotton Fabrics Using $Tio_2$ Nanoparticles

**Sahar Emam[1], Emam Abdel-Mobdy Abdel-Rahim [2], Azza Abd-elAziz Mahmoud[1], Mohamed Abdel-Shakur Ali[2*]**

[1] *Cotton Technology Research Division, Cotton Research Institute, Agriculture Research Center, Giza, Egypt*
[2] *Biochemistry Department, Faculty of Agriculture, Cairo University, Giza, Egypt*

**Abstract**

Titanium dioxide nanoparticles ($TiO_2$-NPs), which are optically active metal nanoparticles that give cotton textiles excellent self-cleaning, UV blocking, and antibacterial performance, are prepared using the sol-gel method to investigate the novel qualities of cotton fabric. Using succinic acid 5 g/L/SHP as an across-linking agent, $TiO_2$-NPs were prepared at two distinct concentrations (1% and 3% OWF) and applied to cotton fabrics (Giza 88 and Giza 94) to investigate the mechanical characteristics, UV-blocking abilities, microorganisms, and self-cleaning capabilities of textile. The characterization of $TiO_2$-NPs was investigated using UV–VIS spectroscopy, Transmission Electron Microscopic (TEM), Energy Dispersive X-ray spectra (EDX) and Zeta potential and particle size. The elemental analysis and surface morphology of treated cotton fabrics are characterized by Fourier transform infrared spectroscopy (FTIR), X-ray diffraction (XRD), and scanning electron microscopy (SEM). Tensile strength and elongation of the treated fabrics are also evaluated. The results showed that the average size of $TiO_2$ nanoparticles was 65.7 nm which has excellent UV protection value (UPF 50+), self-cleaning property, the inhibition zone increased at concentration of 3% for negative and positive bacteria (*Escherichia coli* and *Staphylococcus aureus*). The tensile strength decreased using 1% $TiO_2$-NPs but with increasing the concentration to 3%, the mechanical properties were improved. The results of this investigation demonstrated that the cotton fabric treated with $TiO_2$-NPs exhibited superior general characteristics when compared to the untreated samples. Giza88 was superior to Giza 94, due to the genetic characteristics of the variety.

***Keywords:*** Titanium dioxide nanoparticles, UV protection, Self-cleaning, Antimicrobial, Textiles, Cotton fabrics, X-ray diffraction (XRD), Fourier transform infrared spectroscopy (FTIR).

## 1. Introduction

In recognition of its special qualities such as its softness, affinity for skin, biodegradability, absorbency, and moisture comfort cotton is the most widely used natural fiber in the textile industry **[1]**. Durably functionalizing cellulosic textiles to make them stain-repellent, air-permeable, hydrophobic, electrically conductive, photo-luminescent, self-cleaning, antimicrobial, UV protecting, and pollutant-removing while maintaining comfort is now possible. Novel approaches utilizing a range of functionalizing agents derived from metal salts can accomplish these characteristics such as metal-organic compounds, metal oxides, and metal nanoparticles **[2]**. The process of giving textile materials useful qualities is being revolutionized by nanotechnology **[3]**. Nanotechnology is needed to give cotton, the king of natural fibers, properties like flame retardancy, antimicrobial properties, UV protection, and extreme hydrophobicity. These qualities are also imparted with the aid of nano-finishing, which preserves cotton's natural comfort level. Furthermore, because of its nano-size range, comparatively little material is needed to impart the functional feature **[2,4]**. Due to its remarkable qualities, nanotechnology and nanoscience have become extremely important in recent years **[5]**. Nanoparticles (NPs) have garnered interest in a variety of sectors, including electronics, research, medicine, and environmental cleaning **[6]**. Since of their high surface area-to-volume ratio (SVR) and high surface energy, NPs are becoming more and

*Corresponding author e-mail: mohamed_soliman@cu.edu.eg.;(Ali M.A.), *ORCID:* https://orcid.org/0000-0002-1717-8265
EJCHEM use only: Received date 17 May 2024; revised date 05 July 2024; accepted date 08 July 2024
DOI: 10.21608/ejchem.2024.290333.9731

more in demand since they may be used in a variety of ways **[7]**. The NPs can be divided into two groups according to the elements they contain: metallic and non-metallic **[8]**.

While metal NPs primarily consist of gold (Au), silver (Ag), Titanium (Ti), platinum (Pt), copper (Cu), and Fe (0), metallic NPs also include metal oxides. Titanium dioxide ($TiO_2$) **[9]**, zinc oxide (ZnO) **[10]**, iron oxide ($Fe_2O_3$/$Fe_3O_4$) **[11]**, magnesium oxide (MgO) **[12]**, copper oxide (CuO) **[13]**, alumina ($Al_2O_3$), and numerous other metal oxide nanoparticles are among the metal oxide nanoparticles **[14]**. The synthesis of $TiO_2$-NPs can be achieved by three distinct methods: chemical, physical, and biological. The physical methods include the chemical gas-phase atomic layer deposition (ALD) technique, reactive DC magnetron sputtering, thermal evaporation, pulsed discharge plasma, and pulsed laser deposition (PLD). $TiO_2$-NPs recently employing a pressurized argon atmosphere and high-voltage discharge plasma **[15]**.

Sol-gel synthesis was used by Jongprateep *et al.* **[16]** to create $TiO_2$-NPs with a size range of 48–85 nm. $TiO_2$-NPs were synthesized in this study using titanium (IV) isopropoxide (TTIP) as a precursor. $TiO_2$-NPs have several advantages over other metal oxides, including photo-catalysis, low cost, great abundance, self-cleaning properties, strong oxidizing power, and improved chemical stability **[17]**. Additionally, it has antibacterial, flame-retardant and UV protection qualities when used in textile finishing. $TiO_2$-NPs have a wide surface area, excellent surface morphology, and inherently non-toxic **[2,18]**. Because of the oxygen vacancies, which encourage the growth of positive electrons or $Ti^{3+}$ centers and, as a result, excess e-donors in the electronic structure of titanium, it is an N-type semiconductor **[19]**. According to Žerjav *et al.* **[20]**, the two main disadvantages of using undoped $TiO_2$ as a photo-catalyst are its broadband gap, which ranges from 3.00 to 3.30 eV depending on the polymorph of $TiO_2$ utilized, and high charge carrier recombination rate. Therefore, since $TiO_2$ exhibits photo-catalytic action in the presence of a UV light source, this problem could be resolved by using a UV source. The purpose of this research is to coat cotton fabrics with titanium dioxide nanoparticles, which will enable the fabrics to self-clean and become anti-microbial as well as protect against damaging UV radiation.

While metal NPs primarily consist of gold (Au), silver (Ag), Titanium (Ti), platinum (Pt), copper (Cu), and Fe (0), metallic NPs also include metal oxides. Titanium dioxide ($TiO_2$) **[11]**, zinc oxide (ZnO) **[12,13,14]**, iron oxide ($Fe_2O_3$/$Fe_3O_4$) **[15,16]**, magnesium oxide (MgO) **[17]**, copper oxide (CuO) **[18]**, alumina ($Al_2O_3$), and numerous other metal oxide nanoparticles are among the metal oxide nanoparticles **[19,20]**. The synthesis of $TiO_2$-NPs can be achieved by three distinct methods: chemical, physical, and biological. The physical methods include chemical gas-phase atomic layer deposition (ALD) technique, reactive DC magnetron sputtering, thermal evaporation, pulsed discharge plasma, and pulsed laser deposition (PLD). $TiO_2$-NPs recently employing pressurized argon atmosphere and high-voltage discharge plasma **[21]**.

Sol-gel synthesis was used by Jongprateep *et al.* **[22]** to create $TiO_2$-NPs with a size range of 48–85 nm. $TiO_2$-NPs were synthesized in this study using titanium (IV) isopropoxide (TTIP) as a precursor. $TiO_2$-NPs have a number of advantages over other metal oxides, including photo-catalysis, low cost, great abundance, self-cleaning properties, strong oxidizing power, and improved chemical stability **[23]**. Additionally, it has antibacterial, flame-retardant and UV protection qualities when used in textile finishing. $TiO_2$-NPs have a wide surface area, excellent surface morphology, and are inherently non-toxic **[3,24]**. Because of the oxygen vacancies, which encourage the growth of positive electrons or $Ti^{3+}$ centers and, as a result, excess e-donors in the electronic structure of titanium, it is an N-type semiconductor **[25]**. According to Zheng *et al.* **[26]** and Žerjav *et al.* **[27]**, the two main disadvantages of using undoped $TiO_2$ as a photo-catalyst are its broad band gap, which ranges from 3.00 to 3.30 eV depending on the polymorph of $TiO_2$ utilized, and high charge carrier recombination rate. Therefore, since $TiO_2$ exhibits photo-catalytic action in the presence of a UV light source, this problem could be resolved by using a UV source. The purpose of this research is to coat cotton fabrics with titanium dioxide nanoparticles, which will enable the fabrics to self-clean and become anti-microbial as well as protect against damaging UV radiation.

## 2. Materials and Methods

### 2.1. Materials

Unbleached long stable Egyptian cotton fabrics were purchased from Miser-El-Mhala Company for Spinning and Textile, Egypt, which were created from Giza 88 and Giza 94. The textiles are plan weaved, with a warp of 36 yarns per $cm^2$ and a weft of 30 yarns per $cm^2$, weighing 150 grams. Every experimental material was kept in a controlled atmosphere with a temperature of $25^oC \pm 2^oC$ and a relative humidity of $65^oC \pm 2\%$.

### 2.2. Chemicals

Titanium (IV) isopropoxide,+97% ($C_{12}H_{28}O_4Ti$) was obtained and purchased from Thermo Fisher (Kandel), Germany. Succinic acid 99%, NaOH and

$H_2O_2$ were purchased from PIOCHEM. Sodium hypophosphate (SHP) was obtained from Central Drug House (P) LTD, New Delhi. Reactive (drimen) dye blue 2 ($C_{29}H_{20}ClN_7O_{11}S_3$ was purchased from ICN Biomedical INC., Germany.

### 2.3. Pretreatment processes

*2.3.1. Scouring*

The procedure of scouring was in accordance with Hebeish *et al.* **[21]**. Giza 88 and Giza 94 cotton fabrics were immersed in one liter of an aqueous solution containing 40g/L NaOH (1M) and 1% mercerol (wetting agent) at 100°C for ninety minutes while being constantly stirred. The liquor total ratio will remain at 1:30. Following scrubbing, the samples underwent a thorough washing under running water and then samples were dried.

*2.3.2. Bleaching*

The following bleaching procedure was to bleach fabric in the slack state according to Hebeish *et al.* **[21]** method: The scoured materials were bleached for one hour at 90°C using the silicate ($Na_2SiO_3.9H_2O$) 3.5%, $Na_2CO_3$ 1% and $H_2O_2$ 4%. At a liquor ratio of 20:1, every desiring, scouring and bleaching experiment was run in triplicate.

*2.3.3. Dyeing process*

The altered textiles were colored using reactive (drimen) dye with 6% owf (on fabric weight) at a material-to-liquor ratio of 1:50 using 1% owf. The samples were first submerged in the water, and the dyeing bath was heated to 50°C. The prepared salt was added to the dyeing bath three times, and the dye solution was added. After 15 minutes of boiling, the dyeing was allowed to continue for 45 minutes, at which point it was stopped and the dyeing bath was cooled. Following a thorough rinsing with running water, the dyed samples were soap-soaped for 15 minutes at 70°C in a solution containing 5g/L nonionic detergent (Hostapal CV-ET). After being cleaned, the samples were finally rinsed with water and allowed to dry in air **[22]**.

### 2.4. Treatment Processes

*2.4.1. Preparation of $TiO_2$-NPs*

Titanium tetra isopropoxide (6 mL) and 1% acetic acid (2 mL) were mixed using a magnetic stirrer. After five minutes, two milliliters of strong HCl were added to the solution to adjust its pH, after 56 milliliters of ethanol had been added dropwise while stirring continuously. After 45 minutes of vigorous magnetic swirling of the combination, a viscous solution was created, signifying the formation of $TiO_2$-NPs sol-gel. Abou-Okeil *et al.* **[23]** followed this procedure with two hours of calcination at 450°C and twenty-four hours of drying at 110°C in a muffle furnace.

*2.4.2 Cotton treatment with $TiO_2$-NPs*

Succinic acid (5 g/L) and sodium hypophosphite (4% wt/wt) were dissolved in a 100 mL finishing bath to create $TiO_2$-NPs sol-gel cross-linked on cotton fabric samples. To create a dispersed solution, the prepared solution of $TiO_2$-NPs (1% and 3% owf) was sonicated for 20 minutes. The cotton fabrics were submerged in the prepared solution at room temperature. Ultimately, the treated materials underwent three minutes of drying at 120°C and one minute of curing at 150°C. These procedures completed twofold drying and curing **[24]**.

### 2.5. Characterization of nanoparticles

*2.5.1. UV – VIS spectroscopy*

A PG Instruments Ltd. T80 UV-Vis spectrophotometer was used at the Cotton Research Institute (CRI), Agriculture Research Centre (ARC), Egypt, to study the optical characteristics of $TiO_2$-NPs. UV-VIS spectra were recorded between 300 and 700 nm in wavelength.

*2.5.2. Transmission Electron Microscopy (TEM)*

Utilizing transmission electron microscopy (JEM - 1400, JEOL model), $TiO_2$-NPs were morphologically examined. Cairo University Research Park's (CURP) electronic microscope lab captured the images. $TiO_2$-NPs were put on a carbon grid that had been glow-discharged. The TEM operating system then determined the diameter and shape of the nanoparticle specimens.

*2.5.3. Fourier transforms infra-red spectroscopy studies (FTIR)*

Using a Shimadzu FTIR 8400 Spectrophotometer (National Institute for Standards (NIS)), the FTIR spectrum was acquired to determine the functional groups contained in the samples.

*2.5.4. Particle size and zeta potential*

Particle size and zeta potential of the nanomaterials were measured by photon interconnection spectroscopy and Laser Doppler intensity measuring, respectively, using a Zetasizer® 3000 particulate size description analyzer (Malvern Instruments) in the central lab of NIS, a complementary scientific search institute with analytical services. The mean hydrodynamic diameter was determined by advance analysis after size modification was carried out three times at a 25°C scattering angle and confined for three minutes each time. The automatic water dip cell mode was used to verify the zeta potential adjustment.

### 2.6. $TiO_2$-NPs coated with cotton fabrics: characterization.

*2.6.1. Scanning Electron Microscopy (SEM studies)*

SEM Quanta 250 FEG (Field Emission Gun) combined with an EDX unit (Energy Dispersive X-ray Analyses) at 30 KV accelerating voltage and 14x to 1 million magnification was used to capture images of the nanoparticles.

*2.6.2. X-ray diffraction (XRD)*

The nanoparticle on the textiles was characterized using X-ray diffraction (XRD). Using CuK radiation and λ=1.5406A, XRD patterns were obtained with a Bruker D8 advanced rotaflex diffraction meter.

Crystallinity of cellulose: The XRD crystallinity index (CIXRD) was determined from the height ratio given below using the peak height method for native cellulose, which was created by Segal *et al.* **[25]**.

$$\text{CI}_{\text{XRD}}\ (\%) = \frac{I_{002} - I_{am}}{I_{002}} \times 100$$

Where $I_{002}$ was the intensity of the crystalline and $I_{am}$ the height of the minimum.

## 2.7. Application of $TiO_2$-NPs on cotton fabrics

*2.7.1. UV protection*

Using a Cary 50 solar screen transmission spectrophotometer, the transmissions of UV radiation were measured by AS/NZS 4399(1996)-Sun protective apparel - Evaluation and Classification. According to Sharma *et al.* **[26]**, UPF values were automatically calculated and classified using the Australian Standards Association of Australia standard SAAS/NZS 43399, which stands for Australian / New Zealand Standards, Home bush, Australia, 1996.
The amount of UV light that can pass through a substance determines its UPF. When compared to an unprotected person, UPF indicates how long a wearer of a specific clothing may stay outside in the sun before suffering skin reddening **[28]**.

**Table 1:** UV protection and classification **[27]**

| UV protection | UPF classification | Transmitted UV radiation |
|---|---|---|
| Excellent | 40,45,50,50+ | ≤2.5% |
| Very good | 25,30,35 | 4.1-2.6% |
| Good | 15,20 | 6.7-4.2% |
| Non-ratable | 0,5,10 | >6.7% |

*2.7.2. Anti-bacterial screening test*

Gram-positive *Staphylococcus aureus* (ATCC 6538) and Gram-negative *Escherichia coli* (ATCC 8739) were the two microorganisms employed in the agar plate method as a qualitative test to determine the antibacterial impact of the materials **[29]**.

*2.7.3. Agar plate method*

The bacteriostatic activity was applied in sterile Petri plates. The test organisms, 24-hour broth cultures of *S. aureus* and *E. coli*, were used as inoculums. Using a sterile cotton swab, the test organisms were swabbed all over the surface of the agar plates. The test textiles (fabrics coated with nanoparticles) and the control fabrics were gently pressed against the core of the mat culture. The plates were incubated at 37°C for 18 to 24 hours.

*2.7.4. Self-cleaning property*

Self-cleaning finished goods and experiments The untreated and $TiO_2$-loaded fabric samples were dried and conditioned after being dipped for 15 minutes in a basic blue dye solution (1% owf) for staining. The samples were subjected to a 24-hour exposure to UV light. Fabric samples that had not been treated or that had been loaded with $TiO_2$ were assessed for color strength or K/S value. Degradation of the dye stains directly causes a drop in K/S values **[23,30,31]**. It is determined according to the following relation:
Extent of discoloration (%) = (K/S)a x 100\ (K/S)b where (K/S)a is the color strength after exposure to daylight and (K/S)b is the color strength before exposure to daylight.

*2.7.5. Strength and Elongation*

The tensile stress is expressed as the force per unit linear density of the unstrained specimen. The tensile strength (Kg f) and elongation (%) were measured according to ASTM 5035 **[32]** using Shimadzu Testing Machino-Japan at Textile Metrology Department- National Institute for Standard (NIS-Egypt).

2.8 Statistical analysis

All experiments were independently repeated in triplicates. Results were expressed as mean ± standard error (SE). The statistical analysis was performed in MS Excel and Origin 6.1 software.

## 3. Results and Discussion

The main task of this work is to enhancement of the cotton fabric properties such as UV-protective ability, self-cleaning, and antimicrobial properties by preparing $TiO_2$-NPs and succinic acid as cross-linking agents. Results discuss the size and morphology of the $TiO_2$ nanoparticles and effect on the cotton fabrics.

### 3.1. Characterization of $TiO_2$ -NPs.

*3.1.1. UV – VIS spectroscopy of $TiO_2$-NPs*

The absorption (A) spectrum of $TiO_2$-NPs was measured by Lambada spectrophotometer to find the wavelength peak (lambda max≈316 nm) the absorption spectrum shown in Fig. (1). These results are in agreement with Yang **[33]** which found that the wavelength range of $TiO_2$-NPs between 300-400nm and the optimum particle size of spherical $TiO_2$ is 50-120 nm.

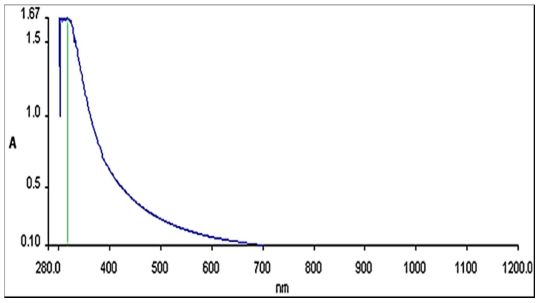


**Figure 1:** UV-VIS spectrum of $TiO_2$-NPs.

*3.1.2. Transmission Electron Microscope (TEM) of $TiO_2$-NPs*

TEM is a useful technique for the analysis of the size and shape of ultrafine particles. Fig. (2) shows the TEM of the prepared $TiO_2$-NPs by sol-gel method. The size and shape of the prepared $TiO_2$-NPs are homogeneous mono-dispersed with some agglomeration. $TiO_2$-NPs were observed to be irregular and hexagonal and the nanoparticle's size displays arrange of 65.7nm **[34]**.

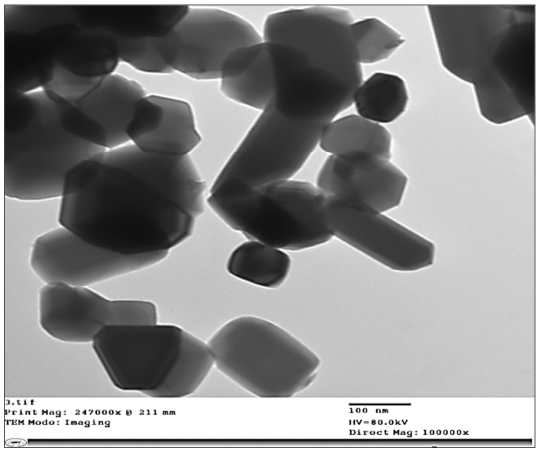


**Figure 2:** Electron micrographs of $TiO_2$-NPs.

*3.1.3. Energy Dispersive X-Ray Spectra (EDX) of $TiO_2$-NPs*

EDX analysis was carried out to verify the composition of the grown nanoparticles. The standard EDX analysis of the grown $TiO_2$-NPs is shown in Fig. (3). The EDX analysis confirms that the grown nanoparticles consist solely of titanium and oxygen, with a percentage of atomic Ti:O of 58.69% compared to 41.31%. Based on EDX and quantitative analysis data, the molecular ratio of Ti:O of the grown nanoparticles was calculated to be nearly that of the bulk. The fact that the spectrum only shows peaks for Ti and O and no other element further indicates that the nanoparticles are made entirely of $TiO_2$ **[35]**.

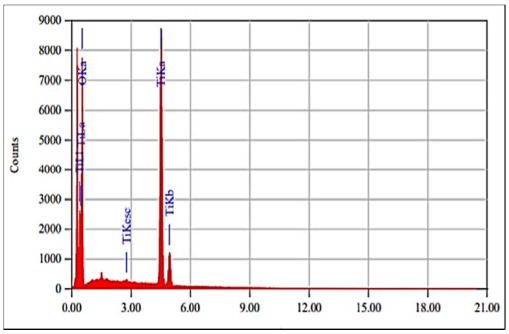


**Figure 3:** Energy Dispersive X-Ray Spectra of $TiO_2$ -NPs.

*3.1.4. Fourier Transform Infrared studies (FTIR).*

Fourier Transform Infrared Analysis of $TiO_2$ -NPs was shown in Fig. (4). The broad band centered at 500-600 $cm^{-1}$ is assigned to the bending vibration (Ti-O-Ti) bonds in the $TiO_2$ lattice. The broad band centered at 3600-3400 $cm^{-1}$ was assigned to the intermolecular interaction of the hydroxyl group for water molecule with $TiO_2$ surface. The peak at 1650 $cm^{-1}$ refers to the characteristic bending vibration of $OH^-$ **[36]**.

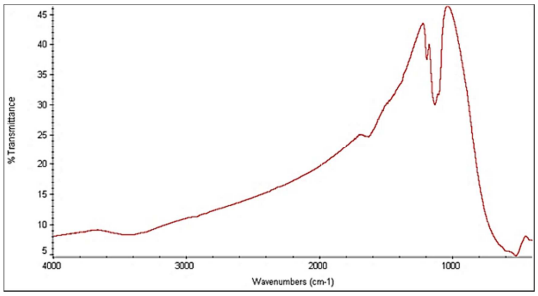


**Figure 4:** Fourier Transform Infrared of $TiO_2$-NPs.

*3.1.5. Zeta potential and particle size.*

Zeta analysis, which is dependent on surface charge, is used to determine the stability of suspended nanoparticles. Particle size and zeta potential of produced $TiO_2$-NPs were investigated according to Rasmussen *et al.* **[37]**. The type of hydrodynamic size (diameter) of produced $TiO_2$-NPs in distilled water was investigated. Fig. (5a) displays the zeta potential for a $TiO_2$-NPs suspension in distilled water. A distinct stability index was observed on zeta potential of -3.14 mV, with an electrophoretic movement (mean) of

0.00253 $cm^2$/Vs. while Fig. (5b) displays the average hydrodynamic diameter of 150 nm for the particle size, These results in agreement with Albukhaty *et al.* **[38]**, who found that the DLS of $TiO_2$-NPs is 150 nm with zeta potential (A) of the opposite value of -44,6mV with electrophoretic movement (mean): 0,000 346$cm^2$/Vs and these findings in agreement with Li *et al.* **[39]**, who found that the prepared suspension confirmed the potential general parameters of zeta negatively to improve stability.

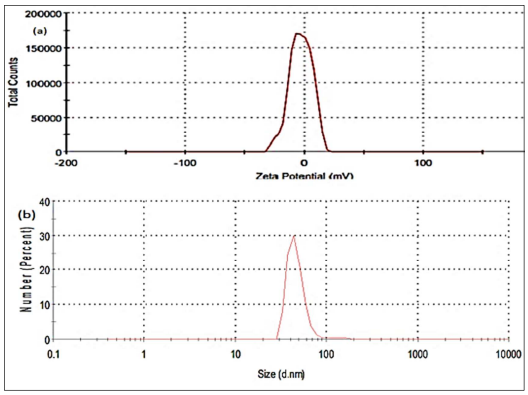


**Figure 5:** (a) Zeta potential and (b) Size distribution by number of $TiO_2$ -NPs.

### 3.2. Characterization of Nano finishing in textiles

*3.2.1. Fourier Transform Infrared studies (FTIR) of cotton fabrics (Esterification with succinic acid)*

Fig. (6a) shows the *FTIR* spectrum of succinic acid. It has been demonstrated that the carboxylic group of succinic acid and the hydroxyl group of cellulose polymer chains can form an ester bond (Fig. 6b). Sodium hypophosphite (SHP) has also been claimed to have the ability to speed up ester formation reactions. It first reacts with an intermediate cyclic anhydride before reacting with cellulose.

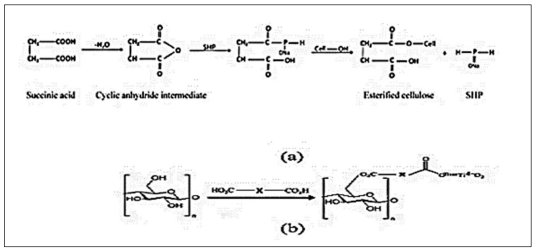


**Figure 6:** (a) Synthesis of $TiO_2$-NPs, cellulose, and dicarboxylic acids (b) Ester covalent and electrostatic bonds, and cyclic anhydride intermediates are formed during the esterification of cellulose with succinic acid **[40]**.

Figs. (7 and 8) display the recorded FTIR spectra for samples (G88 and G94) treated with 5 g/L of succinic acid and 3% of $TiO_2$-NPs. The carbonyl group's (C=O) absorbance peak for esters can be seen between 1700 $cm^{-1}$ and 1750 $cm^{-1}$. The anti-symmetric stretching vibrations of ester carbonyl in carboxyl groups are responsible for the absorption band at 1725 $cm^{-1}$. Regarding the $TiO_2$ spectrum (586 $cm^{-1}$), the peak at 569 $cm^{-1}$ belongs to the Ti–O stretching band. This is explained by the Ti–O covalent connections that develop between cotton fibers and $TiO_2$. It follows that $TiO_2$-NPs interact with cotton fibers **[40]**. This band is visible in every sample that has had carboxylic acid treatment. This suggests that cotton fabric and succinic acid have established ester bonds.

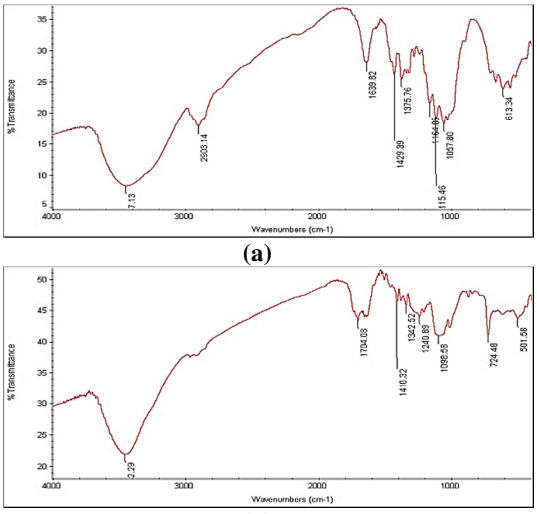


**Figure 7:** FTIR spectrum of cotton fabrics samples (G88) coated with $TiO_2$ -NPs (a) Untreated cotton (b) Treated with $TiO_2$-NPs.

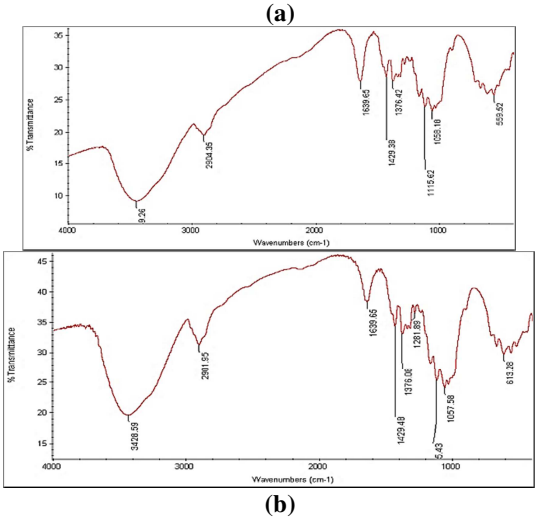


**Figure 8:** FTIR spectrum of cotton fabrics samples (G94) coated with $TiO_2$-NPs (a) Untreated cotton (b) Treated with $TiO_2$-NPs.

*3.2.2. Scanning electron microscope (SEM)*

The surfaces of the treated fabrics were examined using SEM microscopy. The surface morphology of cotton fabric samples (Fig. 9b) treated with $TiO_2$-NPs and bleached cotton fabric (Fig. 9a) is shown in Fig. 9 (a,b). We can see a picture of the delicate and smooth untreated fiber surface in Fig. (9a). However, Fig. (9b) makes it possible to distinguish the $TiO_2$-NPs on the surface of each sample in the treated fabrics. $TiO_2$-NPs attach to the fibers efficiently, adhering to the surface as well as penetrating textile flaws. Additionally, the nanoparticles have a homogeneous distribution throughout the fiber surface, even though some aggregated nanoparticles are still visible. The treated cloth appeared brilliant and white in the SEM images, indicating the presence of white $TiO_2$-NPs on the fabric surface.

The size of the particles affects their ability to adhere to the fibers. The findings are in agreement with those of Saad **[34]** and Azeem *et al.* **[41]** and imply that while the smaller particles will penetrate deeper and adhere strongly to the fabric matrix, the bigger particle agglomerates will be easily removed from the fiber surface. Albukhaty, *et al.* **[38]** explain that sol-gel is one of the most efficient methods for creating $TiO_2$ nanopowder based on their investigation and analysis.

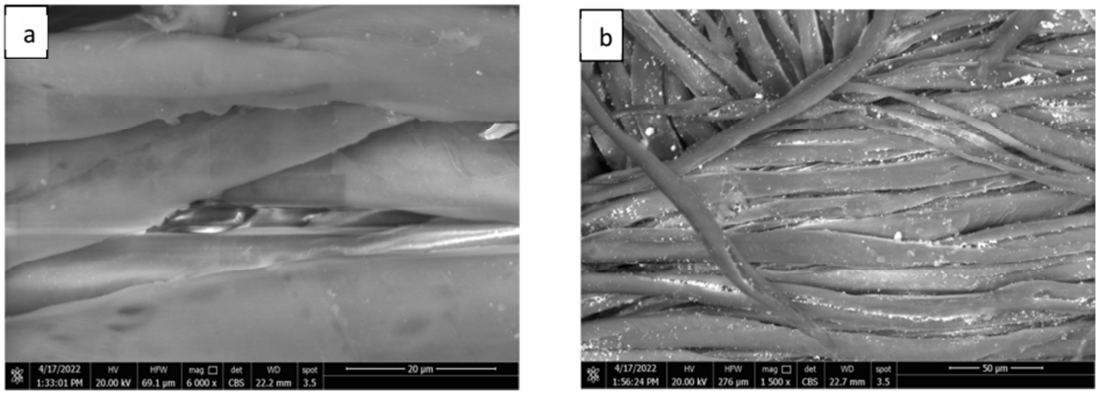


**Figure 9:** SEM of cotton fabric samples coated with $TiO_2$ – NPs (a) Untreated cotton (b) Treated with $TiO_2$ –NPs.

*3.2.3. X-Ray Diffraction Studies*

The substance applied to the fabrics throughout the investigation was examined for crystallinity using XRD studies. Both the applied powder and the substrate's crystallinity are revealed by the XRD pattern. The XRD of cotton fabric G94 and G88 are displayed in Figs. 10 (a,b) and 11 (a,b), respectively. Figures displaying the cotton fabric treated with titanium dioxide XRD graph. Two major peaks can be seen in the graph. The peak at 17 is from cellulose found in all figures, while the peak at 25 is from $TiO_2$-NPs found only in the treated fabrics. This peak confirms the presence of nanoparticles on the fabrics. These results are consistent with Azeem *et al.* **[41]**. The crystallinity index was increased from 76.40 % to 80.88% in the case of G88 and crystallinity index of G94 was increased from 75.42 % to 76.84% in concentration 3% $TiO_2$-NPs which confirmed by the results of tensile strength at concentration 3% these due to the filling of inter yarn spaces in fabric due to this the friction between yarns produced and they resist to elongation and These findings are in agreement with Azeem *et al.* **[41]**.

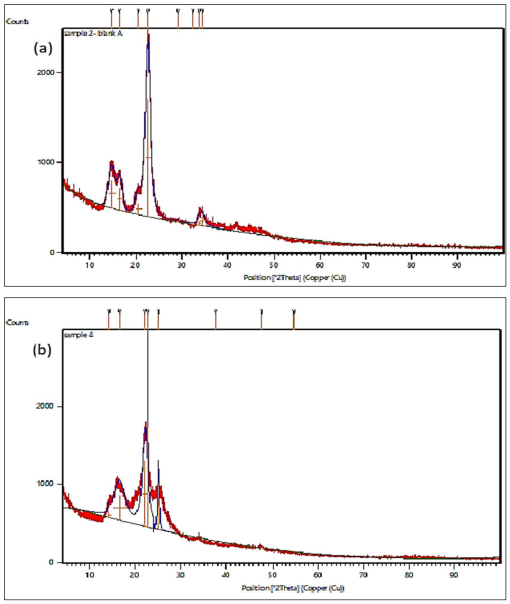


**Figure 10:** XRD studies of cotton fabric samples (G94) coated with TiO2–NPs (a) Untreated cotton (b) Treated with $TiO_2$ –NPs.

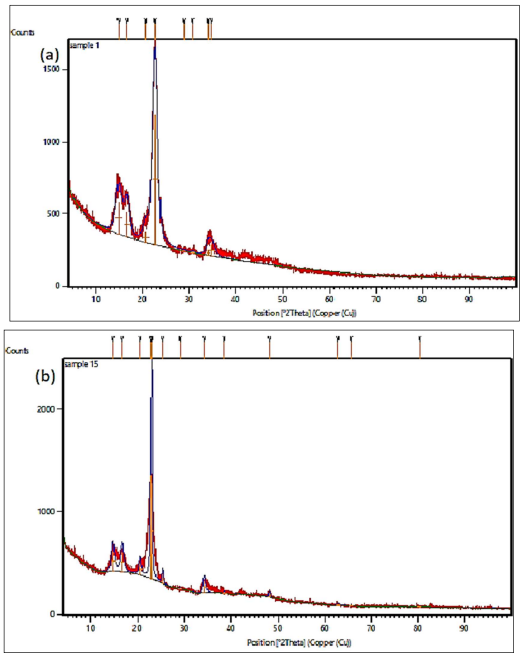


**Figure 11:** XRD studies of cotton fabric samples (G88) coated with $TiO_2$-NPs (a) Untreated cotton (b) Treated with $TiO_2$-NPs.

### 3.3. UV protection properties

The main aim of the current work was to use $TiO_2$-NPs to create a highly UV-absorbing technology that could be used on fabrics. The application of $TiO_2$-NPs with succinic acid/SHP as a cross-linking agent at varying concentrations (1% and 3%), as demonstrated by the results in Table (2).

When compared to untreated cellulose fabrics, treated cellulose fabrics (G88 and G94) showed lower UV transmission. This led to an increase in the automatically calculated UPF (Ultraviolet Protection Factor) value, which indicates how long a person can stay in the sun with special clothing before their skin starts to redden. Table (2) displays the UVA radiation transmitted for cotton fabrics in the UVA (320–400 nm) and UVB (280–320 nm) zones (abbreviated as TUVA and TUVB).

According to the findings, G88 and G94 both suggest a higher UPF value. Excellent UV protection is provided by all treated cotton fabrics. The findings showed that $TiO_2$-NPs treated fabrics could be used for various technological purposes as well as for protecting the skin from sun radiation. Abbas *et al.* **[42]**, and Prorokova *et al.* **[43]** are in agreement with these results of $TiO_2$-NPs.

**Table 2:** Effect of $TiO_2$-NPs with succinic acid on UV protection of cotton fabrics

| | G94 | | | G88 | | |
|---|---|---|---|---|---|---|
| Verities | UPF value | TUVA | TUVB | UPF value | TUVA | TUVB |
| Control | 33.33±3.179797 | 7.29 | 3.03 | 35.86±2.194944 | 5.6 | 3.15 |
| $TiO_2$-NPs 1% | 57.54±3.539371 | 1.71 | 1.65 | 72.04±3.308294 | 2.56 | 1.05 |
| $TiO_2$-NPs 3% | 97±3.997528 | 1.85 | 0.76 | 112.12±4.246667 | 1.18 | 0.68 |

Transmitted UVA (320-400 nm) and UVB (280 -320 nm) regions which were expressed as TUVA and TUVB. UPF: UV protection factor TUV Transmitted UV radiation %. Transmitted UVA (320-400 nm) and UVB (280 -320 nm) regions which were expressed as TUVA and TUVB. UPF: UV protection factor TUV Transmitted UV radiation %. *Each value represents the mean ± standard error, n=3.

### 3.4. Antibacterial properties

The results of the antibacterial test are reported in Tables (3 and 4). The tables show the comparison of antimicrobial activity of the treated fabrics as zone inhibition of bacteria (for the two representative types *S. aureus* and *E.coli* ) for the fabric samples (G88 and G94) treated with two different concentration levels of $TiO_2$-NPs concerning fabric weight such as 1% and 3%. It is clear from the results there is no reduction of bacterial found on the bleaching cotton fabrics but the treated fabric with $TiO_2$-NPs with 1% and 3% show the highest antimicrobial activity against both *S.aureus* and *E.coli* bacterial and response of Giza 88 Variety.

The antibacterial activity of $TiO_2$-NPs in textiles is related to its crystal structure, shape and size. It is based on degrading organic materials by photo-catalytic reaction. Strong chemical reactivity is exhibited by the oxygen and hydroxyl radicals that are formed. Specifically, atomic oxygen reacts with the majority of organic compounds to produce carbon dioxide and water when it reacts with organic compounds in bacteria. Consequently, the bacteria can be eliminated quickly, and textile odors and oil stains can be removed **[38]**.

**Table 3:** Effect of $TiO_2$-NPs with different concentration on zone inhibition of *E.coli*

| Verities | G88 | G94 |
|---|---|---|
| | Inhibition Zone (mm) | |
| Control | 0±.000 | 0±0.00 |
| $TiO_2$-NPs 1% | 10±1.04083 | 9±1.4433 |
| $TiO_2$-NPs 3% | 13±1.2583 | 11±1.5275 |

*Each value represents the mean ± standard error, n=3.

**Table 4:** Effect of $TiO_2$-NPs with different concentration on zone inhibition of *Staphylococcus aureus*

| Verities | G88 | G94 |
|---|---|---|
| | Inhibition Zone (mm) | |
| Control | 0±.000 | 0±0.000 |
| $TiO_2$-NPs 1% | 12±1.607275 | 11±1.322876 |
| $TiO_2$-NPs 3% | 15±1.154701 | 14±1.040833 |

*Each value represents the mean ± standard error, n=3

*3.4.1. Mechanism of antimicrobial activity of $TiO_2$-NPs*

$O_2$-NPs exhibit negative charges on their surface at the point of zero charge (pzc) at pH = 6.2, which indicates a reduced bactericidal effect in neutral and alkaline solutions. This is so because, in these conditions, $TiO_2$-NPs repel microorganisms with a negative charge in the absence of light **[44]**. The $TiO_2$-NPs are positively charged and exhibit significant bacterial cell-to-cell interactions in acidic pH conditions, the bacterial membrane is penetrated, leading to oxidative damage **[45]**. A thorough sequence implicated in $TiO_2$-NPs toxicity to microorganisms is shown in Fig. 12. By adhering to $TiO_2$-NPs on the surface of the microorganism, $TiO_2$ inhibits or eliminates the microbe. Reactive oxygen species (ROS) ($O^{\cdot 2-}$, $OH^{\cdot}$) are formed and initially interact with the lipids on the microorganisms' membrane surface **[46]**. Lipid peroxidation results from the interaction of ROS with the lipids on the membrane. Furthermore, there is an increase in the lipid membrane's permeability. After causing damage to the membrane lipids, the ROS enters the microorganism's cytoplasm and begins to destroy its DNA and ribosomal proteins as well as the nucleus and other cellular organelles. Denaturation of proteins and DNA is caused by ROS oxidizing them. Finally, the microorganisms are killed when the damaged lipid membrane allows all of the damaged cytoplasmic contents to flow out. Prior research has also demonstrated the toxicity of $TiO_2$-NPs on a variety of microorganisms. Kiwi *et al.* **[9]** demonstrated that $TiO_2$-NPs had a bactericidal impact on *Escherichia coli* when they came into close contact with the bacteria in a dark condition. The minus-charged bacterial cell wall at a pH near but below the point of zero charge is attracted to the $TiO_2$-NPs electrostatically, which damages the cell wall during this process. According to Vatansever *et al.* **[47]**, the fundamental source of $TiO_2$-NPs antibacterial action is the formation of ROS when UV light is present. This implies that the bactericidal activity is caused by UV light rather than $TiO_2$-NPs. $TiO_2$-NPs have also shown promise in the destruction of multidrug-resistant bacteria by generating reactive radicals via electron-hole pairs during UV irradiation **[48]**. The power and duration of UV-A light irradiation are critical factors in the inactivation of drug-resistant bacteria by photo-catalytic materials like $TiO_2$-NPs **[49]**. Because of this, the disinfection approach requires a high-power UV source to excite $TiO_2$-NPs, and because of their poor photo-excitation in visible light, there are fewer bactericidal applications. Because of this, $TiO_2$-NPs effectiveness against microbes is restricted in indoor environments with low UV light levels. Therefore, one of the most pressing needs in the medical and industrial sectors is the development of such $TiO_2$-NPs that, in addition to their remarkable antibacterial capabilities, may be activated by visible light.

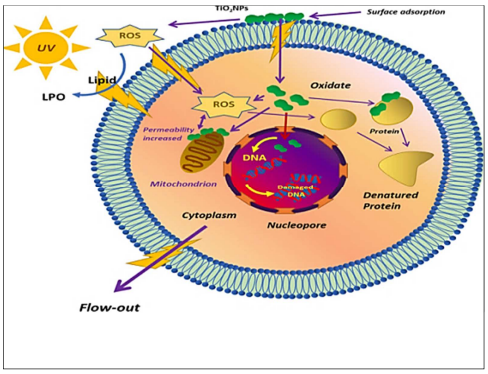


**Figure 12:** Schematic diagram of the toxicity of $TiO_2$NPs to microorganisms **[50]**.

### 3.5. Self-cleaning properties

Cotton fabrics coated with $TiO_2$-NPs were analyzed using the photo-catalytic degradation methylene blue under UV-visible irradiation. Fig. 13 shows the degradation methylene blue of $TiO_2$-NPs on fabrics (G88 and G94) with different concentrations (1% and 3 with respect to the weight fabrics) under UV-visible irradiation at 24 h the data shows that the degradation rate increases with the increasing of $TiO_2$ concentration and irradiation time these results in agreement with Kale *et al.* **[51]**, who found that all $TiO_2$ coated samples show the photo-catalytic properties and capable of stain degradation. Also, the results were in agreement with Alvarez-Amparán *et al.* **[52]**, who found that the $TiO_2$-NPs functionalized cotton fabrics degraded 99% of methylene blue in 60 min by photo-catalysis under UV and solar irradiation conforming self-cleaning properties. Abou-Okeil *et al.* **[23]** found that 2 % of $TiO_2$ nanoparticles are almost sufficient to give enough self-cleaning.

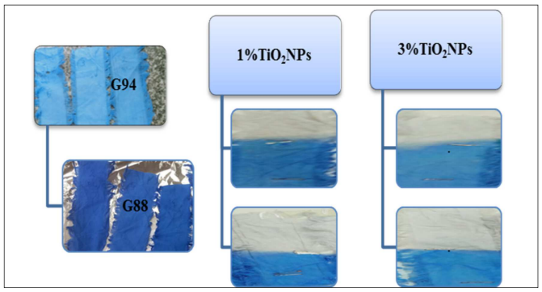


**Figure 13:** Image of methylene blue degradation by $TiO_2$-NPs on cotton fabrics.

*3.5.1. Self- cleaning mechanism of $TiO_2$-NPs*

The fundamental mechanisms of $TiO_2$-NPs photo-catalysis have been the subject of numerous studies **[53-56]**. As previously mentioned in the introduction, heterogeneous photo-catalysis is based on the theory that photon energy either equals or exceeds the band gap (hv ≥ Eg) of a semiconductor, typically $TiO_2$-NPs, upon absorption. As shown in Fig. 14, highly reactive oxygen species (ROS) are generated when the newly formed electron-hole pairs take part in a series of oxidation-reduction events with species adsorbed on the $TiO_2$-NPs surface to generate highly reactive oxygen species (ROS). These organisms cause hazardous pollutants like $CO_2$ and $H_2O$ to break down when they interact with the bacteria or adsorbed organic compounds on the $TiO_2$-NPs surface. However, the shorter half-lifetimes of electrons and holes usually restrict their availability for participation in redox reactions. Moreover, the recombination event is indicated by energy emitted as waste heat or light and a decrease in process efficiency.

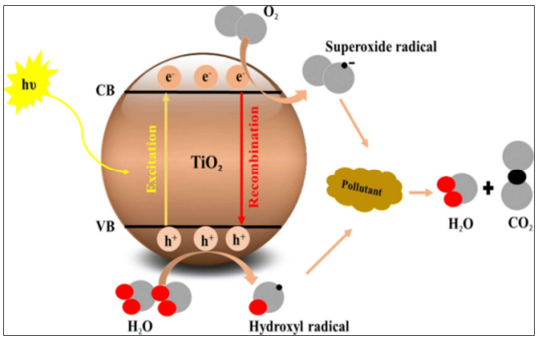


**Figure 14:** TiO2-NPs semiconductor photo-catalysis principle.

## 3.6. Mechanical properties of cotton fabric

*3.6.1. Tensile elongation and strength*

Tensile strength is measuring of fiber strength which depends on the crystal region of the cellulose unit which is observed as a parallel unit that makes a block that makes strength. The mechanical data of the treated and untreated samples were obtained in Table (5). $TiO_2$-NPs treatment with two different concentrations and succinic acid caused increments in fabric strength accompanied by a decreasing in concentration recorded from 420 N in the control sample to 392 N under a concentration 1% then followed slightly increased by concentration of 3% recorded of 423.63 N these in Giza 88.

The same matter in Giza 94 also decreased in concentration recorded from 365.46 N in the control sample to 317 N in concentration of 1% then followed by increasing under concentration of 3%. The decreasing value of tensile strength due to the acidity of succinic acid in the impregnation bath. This leads to an irreversible de-polymerisation of the cellulose molecules **[24]**.

$TiO_2$-NPs exhibit strong photo-catalyst ability; the fiber macromolecules are readily broken, increasing the number of molecular chains in the amorphous portion of the fiber and weakening its supermolecular structure. In the end, this causes the fibers' macro-mechanical properties to decrease. Therefore, during the development and use of nanoscale composite multifunctional textiles, it will be essential to make the nanometer particle equally spread onto the textile and firmly combine it with nanometer material and fiber **[57]**. However, Rahman *et al.* **[58]** discovered that a 2% concentration of $TiO_2$ increased the tensile strength. Further improves the tensile strength because the fabric between spaces are filled, creating friction between the yarns that prevents elongation. These findings concur with those of Azeem *et al.* **[41]**, who discovered that tensile strength improves along with increasing TTIP concentration.

On the other hand Fabric elongation is the increase in length of specimen expressed as a percentage of the original fiber length. Elongation is a property against the strength in which every increase in strength opposite decrease in elongation as shown in Table (5).

$TiO_2$-NPs treatment with two different concentrations and succinic acid 5 g/L leads to an increase in fabric elongation % in Variety G94 which was increased by increasing the concentration relative to control that recorded 19.40 mm and increased in concentration 1% to 25.77 mm then decrease gradually to 24.14 mm by concentration of 3% $TiO_2$ these concentrations have a highest tensile strength.

On the other hand, the elongation % of G88 in the control (untreated cotton fabric) was recorded at 18.33 mm and the treatment of $TiO_2$-NPs with succinic acid led to an increase in concentration 1% recorded at 22.24 mm and then decreased with increased concentration to 3% which recorded 21.02

mm. Sadr and Montazer **[59]** found that The shrinkage that may occur during sonication, causing a slight increase in breaking elongation from 5 to 6%, could be linked to the loss of tensile strength fabric and/or to the cleavage of the cellulosic chains by acid hydrolysis. The results showed that *in situ* sono-synthesis of $TiO_2$-NPs on cotton fabric did not significantly damage the cotton structure. These results are in agreement with Saad **[34]** which found that all treated fabrics with $TiO_2$-NPs showed a decrease in $TiO_2$ nanoparticles can be attributed to those spaces between fibers after treatment decreases.

**Table 5:** Tensile strength and elongation of cotton fabrics G88 and G94

| | T.S (N) | | Elongation (mm) | |
|---|---|---|---|---|
| Treatment | G94 | G88 | G94 | G88 |
| Control | 365.46±19.1796 | 420±22.1435 | 19.40±2.34109 | 18.33±2.3784 |
| $TiO_2$ NPs 1% | 317±22.3960 | 392±23.4591 | 25.77±1.2850 | 22.24±2.9834 |
| $TiO_2$ NPs3% | 375±22.8983 | 423.63±23.3225 | 24.14±2.3140 | 21.02±2.5027 |

*Each value represents the mean ± standard error, n=3.

## 4. Conclusion

Significant functional qualities including antibacterial activity, self-cleaning activity using the methylene blue stain method, and ultraviolet protection factor were evaluated for the $TiO_2$-NPs with succinic acid treated fabric surfaces. All findings demonstrated the best performance at concentrations (3% $TiO_2$-NPs).$TiO_2$-NPs reduced the tensile strength by 1%, but the mechanical characteristics increased when the concentration was raised to 3%. The variety's genetic traits demonstrated that Giza 88 is superior to Giza 94.

## 5. Conflicts of interest

There are no conflicts to declare.

## 6. References


[1] Roy, T. S., Shamim, S. U. D., Rahman, M. K., Ahmed, F., & Gafur, M. A. (2020). The development of ZnO nanoparticle coated cotton fabrics for antifungal and antibacterial applications. Materials Sciences and Applications, 11(9), 601-610.. https://doi:10.4236/msa.2020.119040

[2] Ali, M. A. S., Abdel-Rahim, E. A. M., Mahmoud, A. A. A., & Mohamed, S. E. (2024). Innovative textiles treated with $TiO_2$-AgNPs with succinic acid as a cross-linking agent for medical uses. Scientific Reports, 14(1), 8045. https://doi.org/10.1038/s41598-024-56653-7

[3] Ali, M. A., Abdel-Moein, N. M., Owis, A. S., Ahmed, S. E., & Hanafy, E. A. (2022). Preparation, characterization, antioxidant and antimicrobial activities of lignin and eco-friendly lignin nanoparticles from Egyptian cotton stalks. Egyptian Journal of Chemistry, 65(1), 703-716. https://doi: 10.21608/ejchem.2021.86987.4221

[4] Shaarawy, S. (2019). A review on the development of innovative capabilities in the textile finishing of natural fibers. Egyptian Journal of Chemistry, 62(Special Issue (Part 2) Innovation in Chemistry), 857-579. https://DOI: 10.21608/ejchem.2019.19009.2169

[5] Zanata, L., Tofanello, A., Martinho, H. S., Souza, J. A., & Rosa, D. S. (2022). Iron oxide nanoparticles–cellulose: a comprehensive insight on nanoclusters formation. Journal of Materials Science, 1-12. https://doi: 10.1007/s10853-021-06564-z

[6] Jassal, P. S., Kaur, D., Prasad, R., & Singh, J. (2022). Green synthesis of titanium dioxide nanoparticles: Development and applications. Journal of Agriculture and Food Research, 10, 100361. https://doi: 10.1016/j.jafr.2022.100361

[7] Egbosiuba, T. C., Abdulkareem, A. S., Kovo, A. S., Afolabi, E. A., Tijani, J. O., Auta, M., & Roos, W. D. (2020). Ultrasonic enhanced adsorption of methylene blue onto the optimized surface area of activated carbon: Adsorption isotherm, kinetics and thermodynamics. Chemical engineering research and design, 153, 315-336. https://doi: 10.1016/j.cherd.2019.10.016.

[8] Amari, A., Yadav, V. K., Pathan, S. K., Singh, B., Osman, H., Choudhary, N., & Basnet, A. (2023). Remediation of methyl red dye from aqueous solutions by using biosorbents developed from floral waste. Adsorption Science & Technology, 2023, 1532660. https://doi: 10.1155/2023/1532660

[9] Kiwi, J., Rtimi, S., Sanjines, R., & Pulgarin, C. (2014). $TiO_2$ and $TiO_2$-Doped Films Able to Kill Bacteria by Contact: New Evidence for the Dynamics of Bacterial Inactivation in the Dark and under Light Irradiation. International Journal of Photoenergy, 2014(1), 785037. https://doi: 10.1155/2014/785037

[10] Onyszko, M., Markowska-Szczupak, A., Rakoczy, R., Paszkiewicz, O., Janusz, J., Gorgon-Kuza, A., ... & Mijowska, E. (2022). The cellulose fibers functionalized with star-like zinc oxide nanoparticles with boosted antibacterial performance for hygienic products.

Scientific Reports, 12(1), 1321. https://doi: 10.1038/s41598-022-05458-7

[11] Yadav, V. K., Amari, A., Gacem, A., Elboughdiri, N., Eltayeb, L. B., & Fulekar, M. H. (2023). Treatment of fly-ash-contaminated wastewater loaded with heavy metals by using fly-ash-synthesized iron oxide nanoparticles. Water, 15(5), 908. https://doi: 10.3390/w15050908

[12] Dabhane, H., Ghotekar, S., Zate, M., Kute, S., Jadhav, G., & Medhane, V. (2022). Green synthesis of MgO nanoparticles using aqueous leaf extract of Ajwain (Trachyspermum ammi) and evaluation of their catalytic and biological activities. Inorganic Chemistry Communications, 138, 109270. https://doi: 10.1016/j.inoche.2022.109270

[13] Maliki, M., Ifijen, I. H., Ikhuoria, E. U., Jonathan, E. M., Onaiwu, G. E., Archibong, U. D., & Ighodaro, A. (2022). Copper nanoparticles and their oxides: optical, anticancer and antibacterial properties. International Nano Letters, 12(4), 379-398. https://doi: 10.1007/s40089-022-00380-

[14] Guerra, F. D., Attia, M. F., Whitehead, D. C., & Alexis, F. (2018). Nanotechnology for environmental remediation: materials and applications. Molecules, 23(7), 1760.https://doi: 10.3390/molecules23071760.

[15] Kondo, H., Machmudah, S., Kanda, H., Zhao, Y., & Goto, M. (2022). Synthesis of titanium dioxide nanoparticle by means of discharge plasma over an aqueous solution under high-pressure gas environment. Alexandria Engineering Journal, 61(5), 3805-3820. https://doi: 10.1016/j.aej.2021.08.081

[16] Jongprateep, O., Puranasamriddhi, R., & Palomas, J. (2015). Nanoparticulate titanium dioxide synthesized by sol–gel and solution combustion techniques. Ceramics International, 41, S169-S173. https://doi: 10.1016/j.ceramint.2015.03.193

[17] Yadav, V. K., Khan, S. H., Choudhary, N., Tirth, V., Kumar, P., Ravi, R. K.,& Godha, M. (2022). Nanobioremediation: A sustainable approach towards the degradation of sodium dodecyl sulfate in the environment and simulated conditions. Journal of Basic Microbiology, 62(3-4), 348-360. https://doi: 10.1002/jobm.202100217

[18] Mahmoud, M., Sherif, N., Fathallah, A. I., Maamoun, D., Abdelrahman, M. S., Hassabo, A. G., & Khattab, T. A. (2023). Antimicrobial and self-cleaning finishing of cotton fabric using titanium dioxide nanoparticles. Journal of Textiles, Coloration and Polymer Science, 20(2), 197-202. https://doi: 10.21608/jtcps.2023.188833.1165

[19] Shi, Y., Jiang, K. X., Zhang, T. A., & Zhu, X. F. (2022). Simultaneous and clean separation of titanium, iron, and alumina from coal fly ash in one spot: electrolysis-hydrolysis method. Separation and Purification Technology, 294, 121247. https://doi: 10.1016/j.seppur.2022.121324

[20] Žerjav, G., Žižek, K., Zavašnik, J., & Pintar, A. (2022). Brookite vs. rutile vs. anatase: Whats behind their various photocatalytic activities?. Journal of environmental chemical engineering, 10(3), 107722. https://doi: 10.1016/j.jece.2022.107722

[21] Hebeish, A. R. &Mashoor and Kamel, M. (1970). Effect of pretreatments on some physical and chemical properties of cotton cellulose before and after dyeing during irradiation part1: effect of pretreatment on the photodegradation of cotton. American Dyestuff Reporter, 60: 39-42.

[22] Wang, J., Freeman, H. S., & Claxton, L. D. (2007). Synthesis and mutagenic properties of 4,4′-diamino-*p*-terphenyl and 4,4′-diamino-*p*-quaterphenyl. Coloration Technology, 123(1), 34-38. https://doi.org/10.1111/j.1478-4408.2006.00058.x

[23] Abou-Okeil, A., Eid, R. A. A., & Amr, A. (2017). Multi-functional cotton fabrics using nano-technology and environmentally friendly finishing agents. Egyptian Journal of Chemistry, 60(Conference Issue (The 8th International Conference of The Textile Research Division (ICTRD 2017), National Research Centre, Cairo 12622, Egypt.), 161-169. https://doi: 10.21608/ejchem.2017.5510

[24] Derakhshan, S. J., Karimi, L., Zohoori, S., Davodiroknabadi, A., & Lessani, L. (2018). Antibacterial and self-cleaning properties of cotton fabric treated with $TiO_2$/Pt. http://nopr.niscpr.res.in/handle/123456789/45029 ISSN:0975-1025 (Online); 0971-0426 (Print)

[25] Segal, L. G. J. M. A., Creely, J. J., Martin Jr, A. E., & Conrad, C. M. (1959). An empirical method for estimating the degree of crystallinity of native cellulose using the X-ray diffractometer. Textile research journal, 29(10), 786-794. https://doi.org/10.1177/004051755902901003

[26] Sharma, D. K. & Maheshwar, S. (2001). Effect of dyeing and finishing treatments on sun protection of woven fabrics – A study.Colourage; Annual, 48; p69.

[27] S.A.AS.: Standards Association of Australia, Standard AS/NZS 43399; Australian/New

Zealand Standards, Home bush, Australia. (1996)
[28] AATCC (Technical manual of American association of textile chemistry and colorist method) (2002). 77, 341-343
[29] AATCC (Technical manual of American association of textile chemistry and colorist method) (1974). Test method of antibacterial activity of fabrics, detection of agar plate method 90(52):268-269.
[30] Bozzi, A., Yuranova, T., Guasaquillo, I., Laub, D., & Kiwi, J. (2005). Self-cleaning of modified cotton textiles by $TiO_2$ at low temperatures under daylight irradiation. Journal of Photochemistry and Photobiology A: Chemistry, 174(2), 156-164. https://doi.org/10.1016/j.jphotochem.2005.03.019
[31] Ibrahim, N. A., Amr, A., Eid, B. M., Mohamed, Z. E., & Fahmy, H. M. (2012). Poly (acrylic acid)/poly (ethylene glycol) adduct for attaining multifunctional cellulosic fabrics. Carbohydrate Polymers, 89(2), 648-660. https://doi.org/10.1016/j.carbpol.2012.03.068
[32] A.S.T.M (American Society for Testing and Materials) (1995). (Mechanical properties. D2654-D5035.
[33] Yang, Z. D. (2013). Application of titanium dioxide nanoparticles on textile modification. Advanced Materials Research, 821, 901-905. https://doi.org/10.4028/www.scientific.net/AMR.821-822.901
[34] Saad, M. O. (2021). Efficient Synthesis of $TiO_2$ nanoparticles and its application in natural fabrics printed with Turmeric dyes. Journal of Egyptian Academic Society for Environmental Development. D, Environmental Studies, 22(1), 33-46. https://doi:10.21608/jades.2021.192233
[35] Awad, M. A., Alanazi, M. M., Hendi, A. A., Virk, P., Alrowaily, A. W., Bahlool, T.,& Ibrahim, E. M. (2022). Potential Role of 'Green'Synthesized Titanium Dioxide Nanoparticles in Photocatalytic Applications. Crystals, 12(11), 1639. https://doi.org/10.3390/cryst12111639
[36] Al-Taweel, S. S., & Saud, H. R. (2016). New route for synthesis of pure anatase $TiO_2$ nanoparticles via utrasound-assisted sol-gel method. J. Chem. Pharm. Res, 8(2), 620-626. ISSN : 0975-7384.CODEN(USA) : JCPRC5
[37] Rasmussen, M. K., Pedersen, J. N., & Marie, R. (2020). Size and surface charge characterization of nanoparticles with a salt gradient. Nature communications, 11(1), 2337. https://doi.org/10.1038/s41467-020-15889
[38] Albukhaty, S., Al-Bayati, L., Al-Karagoly, H., & Al-Musawi, S. (2022). Preparation and characterization of titanium dioxide nanoparticles and *in vitro* investigation of their cytotoxicity and antibacterial activity against Staphylococcus aureus and Escherichia coli. Animal Biotechnology, 33(5), 864-870. https://doi.org/10.1080/10495398.2020.1842751
[39] Li, X., Zhu, D., & Wang, X. (2007). Evaluation on dispersion behavior of the aqueous copper nano-suspensions. Journal of colloid and interface science, 310(2), 456-463. https://doi.org/10.1016/j.jcis.2007.02.067
[40] Khajavi, R., & Berendjchi, A. (2014). Effect of dicarboxylic acid chain length on the self-cleaning property of nano-TiO2-coated cotton fabrics. ACS applied materials & interfaces, 6(21), 18795-18799. https://doi.org/10.1021/am504489u
[41] Azeem, A., Abid, S., Sarwar, Z., Iqbal, Z., Khalid, F., Haseeb, M. A., & Saleem, M. J. (2020). Synthesis and application of titanium dioxide nanoparticles on cotton fabrics for UV protection. Journal of Textile and Apparel, Technology and Management, 11(3).
[42] Abbas, M., Iftikhar, H., Malik, M. H., & Nazir, A. (2018). Surface coatings of $TiO_2$ nanoparticles onto the designed fabrics for enhanced self-cleaning properties. Coatings, 8(1), 35. https://doi.org/10.3390/coatings8010035
[43] Prorokova, N., Kumeeva, T., &Kholodkov, I., (2020). Formation of Coatings Based on Titanium Dioxide Nanosolson Polyester Fibre Materials. Coatings. 10(1):82. https://doi.org/10.3390/coatings10010082
[44] Sharma, P., Kumari, R., Yadav, M., & Lal, R. (2022). Evaluation of $TiO_2$ nanoparticles physicochemical parameters associated with their antimicrobial applications. Indian J. Microbiol. 62, 338–350. https://doi:10.1007/s12088-022-01018-9
[45] Pagnout, C., Jomini, S., Dadhwal, M., Caillet, C., Thomas, F., & Bauda, P. (2012). Role of electrostatic interactions in the toxicity of titanium dioxide nanoparticles toward Escherichia coli. Colloids and surfaces B: Biointerfaces, 92, 315-321. https://doi:10.1016/j.colsurfb.2011.12.012
[46] Khan, S. B., Irfan, S., Lam, S. S., Sun, X., & Chen, S. (2022). 3D printed nanofiltration membrane technology for waste water distillation. Journal of Water Process Engineering, 49, 102958. https://doi:10.1016/j.jwpe.2022.102958
[47] Vatansever, F., de Melo, W. C., Avci, P., Vecchio, D., Sadasivam, M., Gupta, A., ... & Hamblin, M. R. (2013). Antimicrobial strategies centered around reactive oxygen species–

bactericidal antibiotics, photodynamic therapy, and beyond. FEMS microbiology reviews, 37(6), 955-989. https://doi: 10.1111/1574-6976.12026

[48] Kubacka, A., Diez, M. S., Rojo, D., Bargiela, R., Ciordia, S., Zapico, I.,& Ferrer, M. (2014). Understanding the antimicrobial mechanism of $TiO_2$-based nanocomposite films in a pathogenic bacterium. Scientific reports, 4(1), 4134. https://doi: 10.1038/srep04134

[49] Tsai, T. M., Chang, H. H., Chang, K. C., Liu, Y. L., & Tseng, C. C. (2010). A comparative study of the bactericidal effect of photocatalytic oxidation by $TiO_2$ on antibiotic-resistant and antibiotic-sensitive bacteria. Journal of Chemical Technology & Biotechnology, 85(12), 1642-1653. https://doi: 10.1002/jctb.2476

[50] Hou, J., Wang, L., Wang, C., Zhang, S., Liu, H., Li, S., & Wang, X. (2019). Toxicity and mechanisms of action of titanium dioxide nanoparticles in living organisms. Journal of environmental sciences, 75, 40-53. https://doi: 10.1016/j.jes.2018.06.010

[51] Kale, B. M., Wiener, J., Militky, J., Rwawiire, S., Mishra, R., Jacob, K. I., & Wang, Y. (2016). Coating of cellulose-$TiO_2$ nanoparticles on cotton fabric for durable photocatalytic self-cleaning and stiffness. Carbohydrate polymers, 150, 107-113. https://doi.org/10.1016/j.carbpol.2016.05.006

[52] Alvarez-Amparán, M. A., Martínez-Cornejo, V., Cedeño-Caero, L., Hernandez-Hernandez, K. A., Cadena-Nava, R. D., Alonso-Núñez, G., & Moyado, S. F. (2022). Characterization and photocatalytic activity of TiO2 nanoparticles on cotton fabrics, for antibacterial masks. Applied Nanoscience, 12(12), 4019-4032. https://doi.org/10.1007/s13204-022-02634

[53] Diaz-Uribe, C. E., Rodríguez, A., Utria, D., Vallejo, W., Puello, E., Zarate, X., & Schott, E. (2018). Photocatalytic degradation of methylene blue by the Anderson-type polyoxomolybdates/$TiO_2$ thin films. Polyhedron, 149, 163-170. https://doi.org/10.1016/j.poly.2018.04.027

[54] MiarAlipour, S., Friedmann, D., Scott, J., & Amal, R. (2018). $TiO_2$/porous adsorbents: Recent advances and novel applications. Journal of hazardous materials, 341, 404-423. https://doi.org/10.1016/j.jhazmat.2017.07.070

[55] Nadimi, M., Saravani, A. Z., Aroon, M. A., & Pirbazari, A. E. (2019). Photodegradation of methylene blue by a ternary magnetic $TiO_2$/$Fe_3O_4$/graphene oxide nanocomposite under visible light. Materials Chemistry and Physics, 225, 464-474. https://doi.org/10.1016/j.matchemphys.2018.11.029.

[56] Nasr, M., Eid, C., Habchi, R., Miele, P., & Bechelany, M. (2018). Recent progress on titanium dioxide nanomaterials for photocatalytic applications. ChemSusChem, 11(18), 3023-3047. https://doi.org/10.1002/cssc.201800874

[57] Li, J., Xie, B., Xia, K., Li, Y., Han, J., & Zhao, C. (2018). Enhanced antibacterial activity of silver doped titanium dioxide-chitosan composites under visible light. Materials, 11(8), 1403. https://doi.org/10.3390/ma11081403

[58] Rahman, M. M., Khalil, E., Solaiman, M., Khan, M. A., Sarkar, J., Abedin, F., & Al Mamun, R. (2015). Investigation on Physico-Chemical Properties of 100% Cotton Woven Fabric Treated with Titanium Dioxide. American Journal of Applied Chemistry, 3(2), 65-68. https://doi.org/10.11648/j.ajac.20150302.15

[59] Sadr, F. A., & Montazer, M. (2014). *In situ* sonosynthesis of nano $TiO_2$ on cotton fabric. Ultrasonics sonochemistry, 21(2), 681-691. https://doi.org/10.1016/j.ultsonch.2013.09.018